Blind Adaptive Energy Estimation for Decorrelating Decision-Feedback CDMA Multiuser Detection Using Learning-Type Stochastic Approximations

Po-Rong Chang, *Member, IEEE,* Chih-Chien Lee, and Chin-Feng Lin

***Abstract*— This paper investigates the application of linear reinforcement learning stochastic approximation to the blind adaptive energy estimation for a decorrelating decision-feedback (DDF) multiuser detector over synchronous code-division multiple-access (CDMA) radio channels in the presence of multiple-access interference (MAI) and additive Gaussian noise. The decision feedback incorporated into the structure of a linear decorrelating detector is able to significantly improve the weaker users' performance by canceling the MAI from the stronger users. However, the DDF receiver requires the knowledge of the received energies. In this paper, a new novel blind estimation mechanism is proposed to estimate all the users' energies using a stochastic approximation algorithm without training data. In order to increase the convergence speed of the energy estimation, a linear reinforcement learning technique is conducted to accelerate the stochastic approximation algorithms. Results show that our blind adaptation mechanism is able to accurately estimate all the users' energies even if the users of the DDF detector are not ranked properly. After performing the blind energy estimation and then reordering the users in a nonincreasing order, numerical simulations show that the DDF detector for the weakest user performs closely to the maximum likelihood detector, whose complexity grows exponentially with the number of users.**

***Index Terms*— CDMA, DDF multiuser detection, stochastic approximation.**

I. Introduction

THE CONVENTIONAL method of detecting a spread-spectrum signal in a multiuser code-division multiple-access (CDMA) channel employs a filter matched to the desired signal [1], [2]. This conventional single-user detector ignores the presence of interfering signals, or equivalently, ignores the cross correlations between the signals of different users. Therefore, the performance of the single-user detector severely degrades when the relative received power of the interfering signal becomes large, i.e., the near–far effects [1]. To tackle this difficulty, there has been an interest in designing the optimum detector for various multiuser CDMA communication systems [2], [4], [5]. The optimum multiuser detection can be carried out by the maximization of a log-likelihood function. Although the optimum multiuser detection is superior to the conventional single-user detector, S. Verdu [6] showed that the optimum detector requires computational complexity which grows exponentially with increasing the number of users. Since a CDMA system could potentially have a large number of users, it may be impractical to implement the optimum detection unless the number of users is quite small.

Hence, there is a need for suboptimum receivers which are robust to near–far effects with a reasonable computational complexity to ensure their practical implementation. Lupas and Verdu [4] introduced a class of suboptimum detectors that are based on linear transformations of a bank of matched filter outputs. The well-known decorrelator is one of the suboptimum multiuser detectors with simple structure whose complexity increases only in proportion to the number of users [4]. The bit error rate (BER) performance of the decorrelator is independent of the interferers' received energies and, hence, is near–far resistant. However, one major drawback of the decorrelator is that it enhances the noise presented in the received signals. Several other suboptimal detectors have been proposed based on the knowledge of (or the ability to accurately estimate) the users' energies. Such schemes exploit the knowledge of the users' energies via some form of successive cancellation of the multiple-access interference (MAI) from the stronger users. These include the multistage detectors that attempt to cancel the MAI at a later stage by utilizing the tentative decisions made in an earlier stage [5]. More significantly, Duel-Hallen [7] introduced multiuser decision feedback receivers that may be used in conjunction with a multistage architecture. Interference from previous symbols of the same user, as well MAI from stronger users, is removed via the use of decision feedback, leading to significant BER performance improvements. Since the decorrelating decision-feedback (DDF) detector requires the knowledge of the received energies of all the users, the BER performance of the DDF detector is significantly degraded when the receiver did not know all the users' energies. Chen and Roy [11] applied a recursive least sequences (RLS) algorithm to estimate a product of a input symbol and its received energy without training data. In this paper, we propose an alternative novel blind estimation technique to estimate all the users' energies using a stochastic approximation algorithm without training data. In order to further improve the speed of convergence, a linear reinforcement learning scheme [17] is conducted to accelerate the stochastic approximation algorithm. In Section V, simulation results show that the blind energy estimation is able to accurately estimate all the users' energies via additive white

Manuscript received August 5, 1996; revised July 13, 1998.

The authors are with the Department of Communication Engineering, National Chiao-Tung University, Hsinchu, Taiwan, R.O.C. (e-mail: pr-chang@cc.nctu.edu.tw).

Publisher Item Identifier S 0018-9545(99)01051-8.

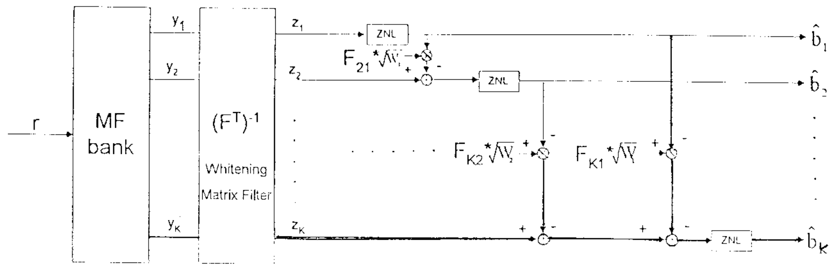

Fig. 1. Block diagram of decorrelating DDF detector.

Gaussian noise (AWGN) channels in the fastest convergence rate and is robust to interfering signals and channel noise.

II. Decorrelating Detectors for Synchronous CDMA Systems

The decorrelating detector is based on an SS-CDMA system with binary phase-shift-keyed (BPSK) signaling [1], [2]. There are a total of K users transmitting over a common wireless channel. Associated with each user $k \in 1, 2, \cdots K$ is a data signal $b_k(t)$ and a signature code waveform $a_k(t)$ which are functions of time. The sampled outputs of a bank of K matched filters at the receiver in the first time interval (reference interval) can be expressed as

$$\boldsymbol{y} = R\boldsymbol{W}\boldsymbol{b} + \boldsymbol{v} \tag{1}$$

where $\boldsymbol{W}$ is a diagonal channel gain or energy matrix with the (k,k)th element $w_{k,k} = \sqrt{W_k}, W_k$ denotes the received energy for user $k, k = 1, 2, \cdots, K, \boldsymbol{y} = [y_1, y_2, \cdots, y_K]^T, \boldsymbol{b} = [b_{1,0}, b_{2,0}, \cdots, b_{K,0}]^T, \boldsymbol{v} = [v_1, v_2, \cdots, v_K]^T$, and v_k is the output of the channel noise $v(t)$ through the kth matched filter. Note that the index "0" in $\boldsymbol{b}$ will be omitted whenever possible. It can be proven that v_k is still a Gaussian noise with zero mean and variance of $N_0/2$, and the covariance matrix of the vector $\boldsymbol{v}$ is

$$E\{\boldsymbol{v}\boldsymbol{v}^T\} = N_0/2R \tag{2}$$

where R is a $K \times K$ positive definite matrix of signature waveform cross-correlation matrix with its (i,j)th element defined as

$$R_{i,j} = \int_0^T a_i(t)a_j(t)\, dt, \qquad i, j \in \{1, 2, \cdots K\}. \tag{3}$$

At an SS-CDMA receiver, the received power from a nearer transmitter can be much bigger than that of a farther transmitter, causing interference and hence degrading the communication quality of a farther transmitter. To tackle the near–far problem [1], a simply decorrelating detector [3] has been proposed to eliminate the near–far problem and then to recover the input data vector $\boldsymbol{b}$ according to the given output vector $\boldsymbol{y}$ without power control. In the decorrelating detector, the matrix filter R^{-1} followed by a set of decision devices (sign detector) is applied to $\boldsymbol{y}$. The output of the matrix filter is

$$\hat{\boldsymbol{y}} = \boldsymbol{W}\boldsymbol{b} + \tilde{\boldsymbol{v}} \tag{4}$$

where $\tilde{\boldsymbol{v}} = [\tilde{v_1}, \tilde{v_2}, \cdots, \tilde{v_K}]^T$ is a Gaussian noise vector with the autocorrelation matrix $E\{\tilde{\boldsymbol{v}}\tilde{\boldsymbol{v}}^T\} = \sigma^2 R^{-1}$.

Then, the detected symbols are obtained by taking the sign detector on each element of $\hat{\boldsymbol{y}}$, i.e.,

$$\hat{\boldsymbol{b}} = \mathrm{sgn}(\hat{\boldsymbol{y}}). \tag{5}$$

The decorrelating detector has several desirable features. It does not require the knowledge of the users' received energies, and its BER performance is independent of the received energies of the interfering users. Hence, the decorrelating detector is near–far resistant. However, one major drawback of the decorrelator is that it enhances the noise presented in the received signals. The power of the noise $\tilde{v_k}$ is $\sigma^2(R^{-1})_{k,k}$, which is greater than noise power σ^2 at the output of the matched filter, where $\sigma^2 = N_0/2$ and $(R^{-1})_{k,k}$ denotes the (k,k)th element of R^{-1}. Thus, the probability that the kth input symbol b_k is recovered incorrectly is given by

$$P_{ek}(Dec) = Q(\sqrt{W_k/[\sigma^2(R^{-1})_{k,k}]}) \tag{6}$$

where the Q function is $Q(x) = 1/\sqrt{2\pi}\ \int_x^\infty\ e^{-y^2/2}\, dy$

III. Bit Error Rate Analysis for Decorrelating DDF Multiuser Detectors with Errors in Estimating Received Energies

Decision-feedback equalizers often have significantly lower BER's than linear detectors in single user channels [7] and have been shown superior to linear detectors in several multiuser systems [5], [7]. Based on this fact, Duel-Hallen [7] has proposed a decorrelating DDF multiuser detector illustrated in Fig. 1 which combines the advantages of both the decorrelating detector and DDF equalizer. It employs forward decorrelating and feedback filters to cancel MAI. The DDF detector cancels MAI completely, provided that the feedback data are decoded correctly. Decisions are made in the order of decreasing received power levels, thus, the weakest user can benefit the most from utilizing the decisions to remove the interference of stronger users. If the received power of the weakest user is significantly lower than that of the other users and the order of the received power levels is correct, the BER performance of the weakest user is close to that of the MAI-free case (single-user bound [7]). On the other hand, the receiver for the stronger user who is the first user in Fig. 1 does not involve feedback and is equivalent to the decorrelator.

In Fig. 1, $(F^T)^{-1}$ is the whitening matrix filter applied to the sampled output of the matched filter bank of (1), where

F is a lower triangular matrix obtained by factorizing the signature waveform cross-correlation matrix as $R = F^T F$ using Cholesky decomposition algorithm. Thus, the resulting output vector is

$$\boldsymbol{z} = F\boldsymbol{W}\boldsymbol{b} + \boldsymbol{n} \tag{7}$$

where $\boldsymbol{n} = [n_1, n_2, \cdots, n_K]^T$ is a white Gaussian vector with the autocorrelation matrix $E\{\boldsymbol{n}\boldsymbol{n}^T\} = \sigma I$, where I is a $K \times K$ identity matrix and $\sigma^2 = N_0/2$. Note that all the components of $\boldsymbol{n}$ are uncorrelated. In addition, it is assumed that the received energies W_k's are known and nonincreasing, i.e., $W_1 \geq W_2 \geq \cdots \geq W_K$. In others words, the strongest user is the first user, and the weakest user is the Kth user.

Duel-Hallen [7] has shown that the BER of the decorrelating decision feedback (DDF) detector for the kth user under the assumption of correct previous decisions is given by

$$P_{ek}^*(\text{DDF}) = Q(F_{k,k}\sqrt{W_k}/\sigma) \tag{8}$$

where $F_{k,k}$ represents the (k,k)th element of F. Since $F_{1,1}^2 = 1/(R^{-1})_{1,1}$, the value of $P_{e1}^*(\text{DDF})$ is identical to that of $P_{ek}(Dec)$ of (6). This implies that the DDF detector for user 1 does not employ feedback and is equivalent to the decorrelating detector. On the other hand, for the weakest user (the Kth user), $F_{K,K}^2 = 1$ and its BER performance is equal to that of the single-user (SU) system given by

$$P_{eK}(SU) = Q(\sqrt{W_K}/\sigma) = P_{eK}^*(\text{DDF}). \tag{9}$$

Actually, the DDF detector does not know the exact values of all the received energies, especially for the time-varying CDMA channel. Thus, the received energies of all the users need to be estimated and updated for proper cancellation of multiuser interference. The general received energy estimation mechanism can be formulated as a mapping from a set of observable parameters in the DDF system to a set of K positive estimated received energies represented by a $K \times 1$ vector, i.e.,

$$G_{ES}\colon V_{ob} \rightarrow (R^+)^K \tag{10}$$

where the space V_{ob} denotes a superset of all the possible observable sets. For example, an observable set may contain the whitening matrix filter outputs $z_i, 1 \leq i \leq K$, the previous estimated energies, and the previous detected symbols. Note that the elements of the observable sets are not unique. Another observable set can be generated from the above-mentioned observable set by replacing the whitening matrix filter outputs z_i's by the matched filter outputs y_i's.

It is desirable to investigate the effect of errors in estimating received energies on the BER performance of a DDF by performing the energy estimator G_{ES}. Assume that the square root value of the estimated energy for the kth user is $\sqrt{\hat{W}_k}$. The kth error pattern for energy estimation is defined as $\triangle W_k = \sqrt{W_k} - \sqrt{\hat{W}_k}$. Therefore, the input to the kth decision device can be derived as follows:

$$\begin{aligned} z_k - \sum_{i=1}^{k-1} F_{k,i}\sqrt{\hat{W}_i}\hat{b}_i &= F_{k,k}\sqrt{W_k}b_k \\ &\quad + \sum_{i=1}^{k-1} F_{k,i}(\sqrt{W_i}(b_i - \hat{b}_i) + \triangle W_i\hat{b}_i) + n_k \end{aligned} \tag{11}$$

where $\hat{b}_i$'s denote the previous detected symbols. If the previous decisions are correct, the remaining interference is resulted from the previous detected symbols and equals $\Sigma_{i=1}^{k-1} F_{k,i}\triangle W_i\hat{b}_i$.

Moreover, the conditional bit error probability for the kth user of a DDF detector with an energy estimator G_{ES} can be found by

$$\begin{aligned} &P_{ek}(\text{DDF} + G_{ES}|b_1, b_2, \cdots b_{k-1}, \hat{b}_1, \hat{b}_2, \cdots, \hat{b}_{k-1}, \\ &\qquad \triangle W_1, \cdots, \triangle W_{k-1}) \\ &\quad = Q\Bigg(F_{k,k}\sqrt{W_k}b_k + \sum_{i=1}^{k-1} F_{k,i}\Bigg(\sqrt{W_i}(b_i - \hat{b}_i) \\ &\qquad + \triangle W_i\hat{b}_i\Bigg)\Bigg/\sigma\Bigg). \end{aligned} \tag{12}$$

Assuming that the input symbols b_i's, the detected symbols $\hat{b}_i$'s, and the energy error patterns $\triangle W_i$'s are mutually independent, their joint probability density function (pdf) can be written as

$$\begin{aligned} &f(b_1, b_2, \cdots, b_{k-1}, \hat{b}_1, \cdots, \hat{b}_{k-1}, \\ &\qquad \triangle W_1, \cdots, \triangle W_{k-1}|G_{ES}) \\ &\quad = f(b_1, b_2, \cdots, b_{k-1}) f(\hat{b}_1, \cdots, \hat{b}_{k-1}) \\ &\qquad \cdot f(\triangle W_1, \cdots, \triangle W_{k-1}|G_{ES}) \end{aligned} \tag{13}$$

where $f(\triangle W_1, \cdots, \triangle W_{k-1}|G_{ES})$ is the pdf of the first $k-1$ energy error patterns conditioned on a specific energy estimator G_{ES}. Hence, the BER for the kth user of a DDF with G_{ES} can be derived as follows:

$$\begin{aligned} &P_{ek}(\text{DDF}|G_{ES}) \\ &\quad = \int_{b_1} \cdots \int_{b_{k-1}} \int_{\hat{b}_1} \cdots \int_{\hat{b}_{k-1}} \int_{\triangle W_1} \cdots \int_{\triangle W_{k-1}} \\ &\qquad \cdot P_{ek}(\text{DDF} + G_{ES}|b_1 \cdots \triangle W_{k-1}) \\ &\qquad \cdot f(b_1, b_2, \cdots, b_{K-1}) \\ &\qquad \cdot f(\hat{b}_1, \cdots, \hat{b}_{k-1}) \\ &\qquad \cdot f(\triangle W_1, \cdots, \triangle W_{k-1}|G_{ES})\, db_1 \cdots db_{k-1} \\ &\qquad \cdot d(\hat{b}_1) \cdots d(\hat{b}_{k-1}) d(\triangle W_1) \cdots d(\triangle W_{k-1}) \\ &\quad = E_{b_1, \cdots b_{k-1}, \hat{b}_1, \cdots \hat{b}_{k-1}, \triangle W_1, \cdots \triangle W_{k-1}} \\ &\qquad \cdot \Bigg\{Q(F_{k,k}\sqrt{W_k}b_k + \sum_{i=1}^{k-1} F_{k,i}(\sqrt{W_i}(b_i - \hat{b}_i) \\ &\qquad + \triangle W_i\hat{b}_i)/\sigma)\Bigg\}. \end{aligned} \tag{14}$$

Since the explicit expression of $f(\triangle W_1, \cdots, \triangle W_{k-1}|G_{ES})$ is actually unknown, it is impossible to derive the exact explicit expression of BER of (14). Although this probability does not have the exact analytical formulation, computer numerical simulations are most commonly used in determining the BER and the effects of energy error propagation.

Equation (14) shows that the BER is highly dependent on the estimation performance of the energy estimator G_{ES}. If G_{ES} is the ideal energy estimator, the energy error patterns $\triangle W_i$'s become zero, and then the BER $P_{ek}(\text{DDF}|G_{ES})$ of

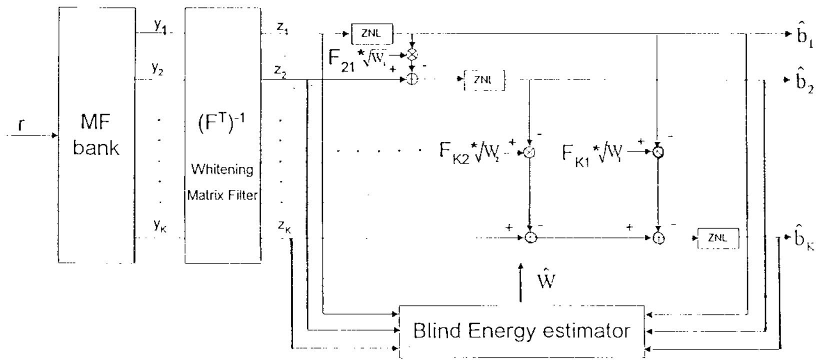

Fig. 2. Block diagram of BDDF detector with blind energy estimator.

(14) is identical to the BER $P_{ek}(\text{DDF}|\text{Ideal Estimation})$ of an ideal DDF with exactly known received energies (ideal estimation). According to the above discussion, the problem of finding the best energy estimator G_{ES}^* can be expressed as an optimization problem given by

$$\min_{G_{ES}} \left[\sum_{k=1}^{K} (P_{ek}(\text{DDF}|G_{ES}) - P_{ek}(DDF|\text{Ideal Estimation}))^2 \right]. \quad (15)$$

IV. Blind Energy Estimation for DDF Multiuser Detectors Using Stochastic Approximation Algorithms with Linear Reinforcement Learning

As mentioned in the above section, the best energy estimator G_{ES}^* can be found by minimizing the cost functional of (15) directly. Since the explicit expression of this cost functional is actually unknown and very complex, it is difficult to find its optimal solution directly. To overcome this difficulty, an alternative expression of cost functional is presented in this section. This expression is found to be particularly suitable for stochastic approximation algorithm without requiring the exact knowledge of unknown probability distribution on each variable. The new energy estimator based on minimizing the alternative cost functional and together with the DDF does not require any training sequence, and its behavior is quite similar to that of Bussgang-type blind equalization [13]. In Section V, simulation results show that the optimal solutions to both the cost functionals result in almost the same optimal performance. On the other hand, the cost functional of (15) is able to provide the performance index to evaluate the solution derived from our alternative cost functional in the BER manner. Fig. 2 shows the basic structure of the DDF detector with a blind energy estimator, where the whitening matrix filter outputs $z_i, 1 \le i \le K$ and the previous detected symbols $\hat{b}_i, 1 \le i \le K$ are the observable and measurable parameters used for the estimator. To implement this estimator, the whitening matrix filter outputs of (7) of the DDF detector should be rewritten as an expression in terms of a $K \times 1$ vector of received energies, i.e.,

$$\boldsymbol{z} = F\boldsymbol{W}\boldsymbol{b} + \boldsymbol{n} = FB\boldsymbol{w} + \boldsymbol{n} \quad (16)$$

where $\boldsymbol{w} = [\sqrt{W_1}, \sqrt{W_2}, \cdots, \sqrt{W_K}]^T$ and $B = \text{diag}(b_1, b_2, \cdots, b_K)$ denotes the $K \times K$ diagonal matrix of input data symbols. Note that $\boldsymbol{w}$ is called the energy vector, where the kth element of $\boldsymbol{w}$ is actually the square root value of the received energy for user k.

An estimate of the whitening filter output vector $\boldsymbol{z}$ is defined by

$$\hat{\boldsymbol{z}} = F\hat{B}\boldsymbol{w} \quad (17)$$

where $\hat{B} = \text{diag}(\hat{b}_1, \hat{b}_2, \cdots, \hat{b}_K)$ denotes the $K \times K$ diagonal matrix of previous detected symbols.

The true K-dimensional energy vector $\boldsymbol{w}^*$ can be found by minimizing the mean-square error (MSE) criterion

$$\begin{aligned} J_E(\boldsymbol{w}) &\triangleq E\{\|\boldsymbol{z} - \hat{\boldsymbol{z}}\|^2\} \\ &\triangleq E_{z_1,\cdots,z_K,\hat{b}_1,\cdots,\hat{b}_K}\{\|\boldsymbol{z} - F\hat{B}\boldsymbol{w}\|^2\}. \end{aligned} \quad (18)$$

By letting the gradient $\nabla_{\boldsymbol{w}} J_E(\boldsymbol{w})$ be a zero vector, the value of the optimal solution $\boldsymbol{w}^*$ is given by

$$\begin{aligned} \boldsymbol{w}^* &= [E\{\hat{B}^T F^T F \hat{B}\}]^{-1} E\{\hat{B}^T F^T \boldsymbol{z}\} \\ &= [E\{\hat{B} R \hat{B}\}]^{-1} E\{\hat{B} F^T \boldsymbol{z}\} \end{aligned} \quad (19)$$

where $E\{\cdot\}$ denotes an expectation over $z_1, \cdots, z_K, \hat{b}_1, \cdots, \hat{b}_K, R = F^T F$, and $\hat{B}^T = \hat{B}$. Since $J_E(\boldsymbol{w})$ is a quadratic polynominal function in terms of $\boldsymbol{w}$, the optimal solution $\boldsymbol{w}^*$ of (19) is the unique global minimum point to (18).

However, the joint probability density function of $z_1, z_2, \cdots, z_K, \hat{b}_1, \hat{b}_2, \cdots, \hat{b}_K$ is actually unknown and very complex. This implies that the optimal energy vector $\boldsymbol{w}^*$ cannot be obtained from (19) directly. Fortunately, Robbins and Monro [14] suggested the following scheme called the stochastic approximation without the evaluation of the expectation over $z_1, \cdots, z_K, \hat{b}_1, \cdots \hat{b}_K$ to solve the gradient of (19) recursively as time evolves:

$$\begin{aligned} \boldsymbol{w}_{i+1} &= \boldsymbol{w}_i - \frac{r_i}{2} \nabla_{\boldsymbol{w}} \{J(\boldsymbol{w}_i)\} \\ &= \boldsymbol{w}_i + r_i \{(F\hat{B})^T (\boldsymbol{z} - F\hat{B}\boldsymbol{w}_i)\} \end{aligned} \quad (20)$$

where $\{r_i\}$ is a learning-rate sequence of positive scalars tending to zero and $J(\boldsymbol{w}) = \|\boldsymbol{z} - F\hat{B}\boldsymbol{w}\|^2$ is the MSE measure which depends on the observed random samples $\{\boldsymbol{z}, \hat{B}_i\}$ and can be treated as the estimate of $J_E(\boldsymbol{w}) = E\{J(\boldsymbol{w})\}$. In other words, the stochastic approximation estimates the unknown deterministic gradient $\nabla_{\boldsymbol{w}} J_E(\boldsymbol{w})$ with the known random gradient $\nabla_{\boldsymbol{w}} J(\boldsymbol{w})$ at each iteration in the discrete stochastic gradient-descent algorithm of (20), where the unknown gradient $\nabla_{\boldsymbol{w}} J_E(\boldsymbol{w})$ points in the direction of steepest descent on the unknown expected-error surface defined by $J_E = E\{J\}$.

The learning-rate coefficients $\{r_i\}$ decrease with time i to suppress random disturbances. In addition, simulation results show that the decreasing coefficients are also able to suppress both the MAI and channel noise. If the sequence $\{r_i\}$ satisfies the conditions of Dvoretzky's theorem [15]

$$\lim_{i\to\infty} r_i = 0, \quad \lim_{n\to\infty} \sum_{i=1}^{n} r_i = \infty$$
$$\lim_{n\to\infty} \sum_{i=1}^{n} r_i^2 < \infty. \tag{21}$$

Then, the random energy vector $\boldsymbol{w}_i$ in (20) converges to the optimal solution to the unknown expected-error function $J_E(\boldsymbol{w})$ of (18) with probability one, i.e.,

$$P_r\left\{\lim_{i\to\infty} \boldsymbol{w}_i = \boldsymbol{w}^*\right\} = 1 \tag{22}$$
$$\lim_{i\to\infty} E\{\|\boldsymbol{w}_i - \boldsymbol{w}^*\|^2\} = 0. \tag{23}$$

It is obvious that the harmonic sequence $\{1/i\}$ satisfies all the three conditions of (21) and can be used as a special case of $\{r_i\}$. Another scheme may be generated by minimizing upper bounds on the variance of the estimated MSE, i.e.,

$$u_i^2 \geq E\{\|\boldsymbol{w}_i - \boldsymbol{w}^*\|^2\}. \tag{24}$$

An optimal sequence of learning rate which satisfies (21) can be generated by

$$r_i^* = \frac{1}{i + \sigma^2/u_1^2} \tag{25}$$

which minimizes the upper bound of the error bound [16]

$$u_{i+1}^2 \leq \frac{\sigma^2}{i + \sigma^2/u_1^2}. \tag{26}$$

The sequence $\{r_i^*\}$ satisfies the Rao-Cramér inequality. This implies that its convergence cannot be faster than at $c_1/(i + c_2)$ where c_1 and c_2 are positive constant numbers. Since this is a serious limitation on the speed of convergence, an acceleration scheme with learning capability has been proposed to accelerate the convergence of the algorithm and would be presented in the next section.

A. Acceleration of Stochastic Approximation Algorithms Using Linear Reinforcement Learning

Saridis [17] has proposed a learning scheme which provides a memory to the multidimensional stochastic approximation algorithms in order to utilize the accumulated past experience of the search for acceleration proposes. In addition, a matrix gain has been used instead of the scalar learning rate r_i. The learning scheme is used to update the weighting coefficients of the new matrix gain applied to the components of the correction terms as to direct the search along the ridge of the expected-error surface defined by J_E and thus accelerate the convergence of the algorithm.

The learning algorithm introduces the weighting matrix $P(i)$ and modifies the gradient-type stochastic approximation algorithm of (20) as follows:

$$\begin{aligned}\boldsymbol{w}_i &= \boldsymbol{w}_{i-1} - \frac{r_i}{2} P(i) \nabla_{\boldsymbol{w}} \{J(\boldsymbol{w}_{i-1})\} \\ &= \boldsymbol{w}_{i-1} + r_i P(i)\{(F\hat{B}_{i-1})^T(\boldsymbol{z}_i - F\hat{B}_{i-1}\boldsymbol{w}_{i-1})\} \\ &= \boldsymbol{w}_{i-1} + r_i P(i)\hat{B}_{i-1}(F^T\boldsymbol{z}_i - R\hat{B}_{i-1}\boldsymbol{w}_{i-1})\end{aligned} \tag{27}$$

where r_i satisfies conditions of (21), and the matrix gain $P(i)$ is defined by

$$P(i) = K \cdot \begin{bmatrix} p_1(i) & 0 & \cdots & 0 \\ 0 & p_2(i) & \cdots & 0 \\ \vdots & \vdots & & \\ 0 & 0 & \cdots & p_K(i) \end{bmatrix}$$
$$0 \leq p_k(i) \leq 1, \qquad p_k(0) = 1/K,$$
$$k = 1, 2, \cdots K$$
$$K \sum_{k=1}^{K} p_k(i) = \mathrm{tr}\{P(i)\} = K, \qquad i = 1, 2, \cdots. \tag{28}$$

A linear reinforcement learning [17] is used to update at every iteration the components of $P(i)$ and alter the direction of the search accordingly

$$p_k(i) = \alpha p_k(i-1) + (1-\alpha)\lambda_k(i) \tag{29}$$

where the rate of learning α and the limiting value $\lambda_k(i)$ of the kth weighting component $p_k(i)$ are defined as follows:

$$0 < \alpha < 1$$
$$\lambda_k(i) = \begin{cases} \varepsilon, & \dfrac{\partial J(\boldsymbol{w}_{i-2})}{\partial w_k} \dfrac{\partial J(\boldsymbol{w}_{i-1})}{\partial w_k} \leq 0 \\ \dfrac{1}{m}, & \dfrac{\partial J(\boldsymbol{w}_{i-2})}{\partial w_k} \dfrac{\partial J(\boldsymbol{w}_{i-1})}{\partial w_k} > 0, k = 1, \cdots, K \\ \dfrac{1}{K}, & m = 0 \end{cases} \tag{30}$$

where $0 \leq m \leq K$ is the number of components of $\nabla J(\boldsymbol{w}_{i-1})$ that did not change sign at the last step. Note that if all the components change sign $(m = 0)$, then

$$\lambda_k(i) = \frac{1}{K}, \qquad k = 1, 2, \cdots, K, \qquad m = 0. \tag{31}$$

In addition, the expression of $\partial J(\boldsymbol{w}_{i-1})/\partial w_k$ can be derived as follows:

$$\begin{aligned}\frac{\partial J(\boldsymbol{w}_{i-1})}{\partial w_k} &= -\boldsymbol{e}_k^T(F\hat{B}_{i-1})^T(\boldsymbol{z}_{i-1} - F\hat{B}_{i-1}\boldsymbol{w}_{i-1}) \\ &= -\boldsymbol{e}_k^T\hat{B}_{i-1}(F^T\boldsymbol{z}_{i-1} - R\hat{B}_{i-1}\boldsymbol{w}_{i-1})\end{aligned} \tag{32}$$

where $\boldsymbol{e}_k = [0, 0, \cdots, 1, 0 \cdots 0]^T$ is a $K \times 1$ vector which contains the zero components except its kth component is an identity.

The above-mentioned iterative algorithm of (27)–(30) is activated only in the presence of a sharp ridge by detecting the successive overshooting of the projected local minimum in the direction of one or more of the coordinate axes. In that case, the projection of the gradient in this direction is penalized while the other projections are reinforced in such a way that the $(i+1)$th step will not be in the direction of the local gradient, but at a direction approaching to the direction of the ridge. The increments being applied at a direction closer to the direction of the ridge will take the search to a region close to the extremum much faster than the conventional gradient-type stochastic approximation algorithm. On the other hand, (31) indicates that the search is moved away from the region of ridge. Moreover, in case of absence of a ridge, no overshooting will occur. Thus, $P(i) = I, i = 1, 2 \cdots$ and the learning-type algorithm degenerates to the conventional stochastic approximation algorithm of (20). More details of learning-type algorithms can be found in [17].

B. Two-Phase Blind Adaptation

Usually, the users in the DDF detector may be not ranked properly according to their received energies. In this case, the first phase blind adaptation is used to identify the order of all the users' received energies within a fixed short time period by using the proposed energy estimation mechanism. After the first phase adaptation, it is desired to sort the energy estimates in a nonincreasing order $\hat{W}_{(1)} \geq \hat{W}_{(2)} \geq \cdots \geq \hat{W}_{(K)}$, where the notation $(\cdot)$ in the subscript denotes the reordered sequence. The second phase adaptation is applied to the reordered users with a proper nonincreasing order and then to obtain the desired detected symbols.

V. Simulation Results

For simplicity, the CDMA channel models used in evaluating the estimation performance of the proposed blind adaptive energy estimator are on the basis of both the two-user and four-user synchronous CDMA AWGN channels with two different signature waveform cross-correlation matrices. The two-user CDMA system is simple and illustrative of the salient features of the blind adaptive energy estimation for the DDF detectors. The first two-user CDMA system contains two signature waveforms, of length three, i.e., $a_1(t) = [1, 1, 1]$ and $a_2(t) = [1, -1, 1]$, which have been previously considered in the literature [5] and correspond to the cross correlation $R_{1,2} = 1/3$. The learning-rate coefficients of learning-type stochastic approximation (LSA) are the harmonic sequence $\{r_i = (1/i)\}$. The rate of linear reinforcement learning is $\alpha = 0.9$. The values of both the weight coefficients and limiting values at the initial step are set to $p_k(0) = (1/2)$ and $\lambda_k(0) = 0, k = 1, 2$, respectively. Assume that the unknown received energies (actually square root values of received energies) for both users 1 and 2 are set to $w_1 = \sqrt{10}$ and $w_2 = 1$, respectively. For simplicity, the square root energy is called the energy in this paper. The variance of AWGN noise is $\sigma^2 = 0.079\,43$. The initial estimated received energies are all set to zero. Fig. 3 illustrates the convergence of two estimated received energies achieved by blind adaptive energy estimation using both the learning-type stochastic approximation (LSA) algorithm and least mean square (LMS) algorithm with two different learning rates $r = 0.05$ and $r = 0.005$ when $w_1 = \sqrt{10}$, $w_2 = 1$, and $\sigma^2 = 0.079\,43$. From Fig. 3, it is observed that the learning curves for both the received user energies achieved by LSA converge to their corresponding respective desired energies, $\sqrt{10}$ and one rapidly. In addition, a comparison of the learning curves in Fig. 3 indicates that LSA converges to the desired energy much faster than LMS. For LMS with a larger rate $r = 0.05$, it results in faster convergence speed, but has a lager variation around the desired energy. On the other hand, the decreasing learning coefficients of LSA are able to suppress the random variation. Thus, no variations occur in the learning curves of LSA. An alternative approach to evaluate the estimation performance is in terms of the following MSE criterion given by:

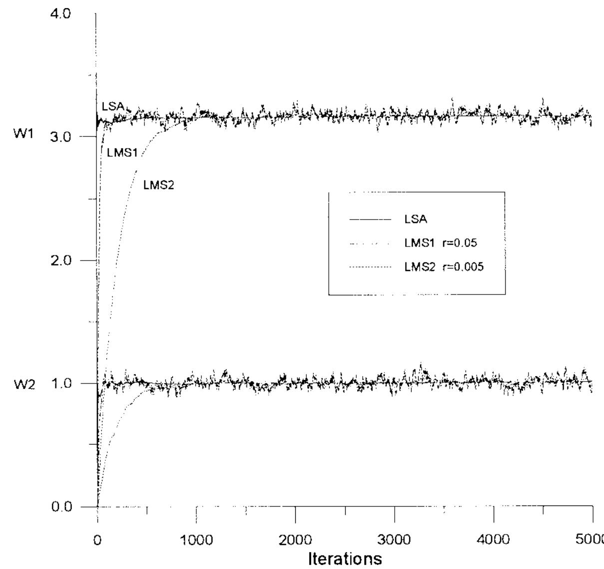

Fig. 3. Comparison of the estimated energies achieved by LSA, LMS1, and LMS2 for a two-user CDMA BDDF detector with $R_{12} = 1/3$ when $w_1 = \sqrt{10}$, $w_2 = 1$, (correct user order), and $\sigma^2 = 0.079\,43$.

$$\text{Error} = E\{\|\boldsymbol{w} - \hat{\boldsymbol{w}}\|^2\} \approx \frac{1}{N} \sum_{m=1}^{N} \|\boldsymbol{w}_{m,\exp} - \hat{\boldsymbol{w}}_{m,\exp}\|^2 \quad (33)$$

where $\hat{\boldsymbol{w}}_{m,\exp}$ is the estimated energy vector obtained from the mth experiment $1 \leq m \leq N$ and N denotes the total number of experiments. Each experiment is generated by a set of randomly chosen binary input symbols. In practice, N is set to 20. The value of MSE is obtained over 20 experiments. Fig. 4 shows the MSE convergence of both the LSA and LMS algorithms with either $r = 0.05$ or $r = 0.005$. Results show that the steady-state value of average error produced by the LSA converges to a value $(\leq 10^{-2})$ rapidly, which is much lower than that of the LMS algorithm with either $r = 0.05$ or $r = 0.005$. These results would be conducted to verify the optimal convergence capability of LSA algorithm.

Next, it is desired to investigate the estimation performance of blind adaptive energy estimation mechanism applied to the DDF detector with the order of users interchanged, i.e., $w_1(= 1) < w_2(= \sqrt{10})$. Figs. 5 and 6 show the convergence of the estimated received energies and their associated MSE errors. It is observed that the blind adaptive energy estimator

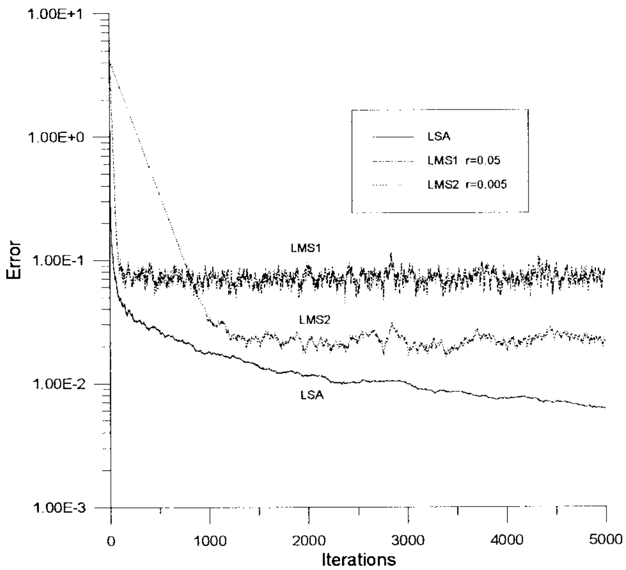

Fig. 4. Comparison of mean square errors achieved by LSA, LMS1, and LMS2 for a two-user CDMA BDDF detector with $R_{12} = 1/3$ when $w_1 = \sqrt{10},\ w_2 = 1$, (correct user order), and $\sigma^2 = 0.07943$.

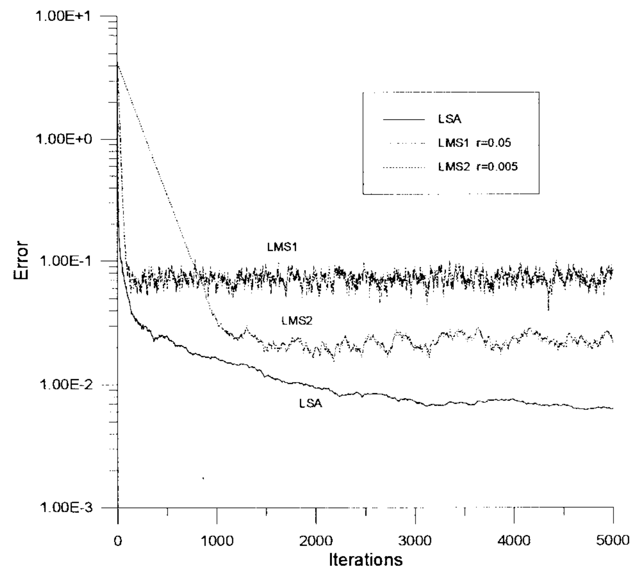

Fig. 6. Comparison of mean square errors achieved by LSA, LMS1, and LMS2 for a two-user CDMA BDDF detector with $R_{12} = 1/3$ when $w_1 = 1,\ w_2 = \sqrt{10}$, (reverse user order), and $\sigma^2 = 0.07943$.

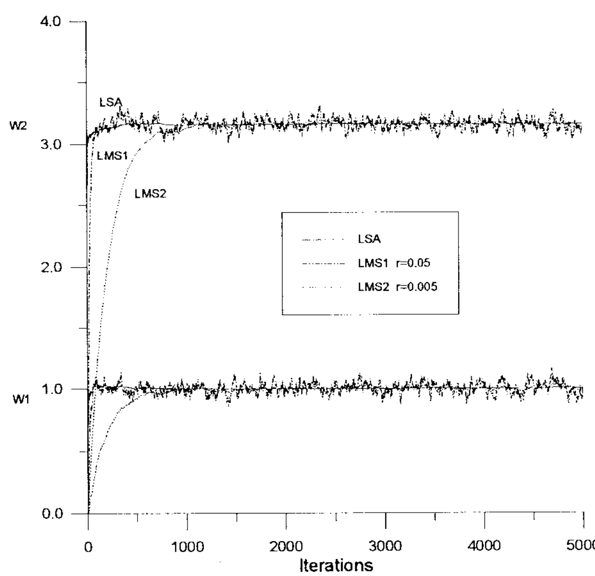

Fig. 5. Comparison of the estimated energies achieved by LSA, LMS1, and LMS2 for a two-user CDMA BDDF detector with $R_{12} = 1/3$ when $w_1 = 1,\ w_2 = \sqrt{10}$, (reverse user order), and $\sigma^2 = 0.07943$.

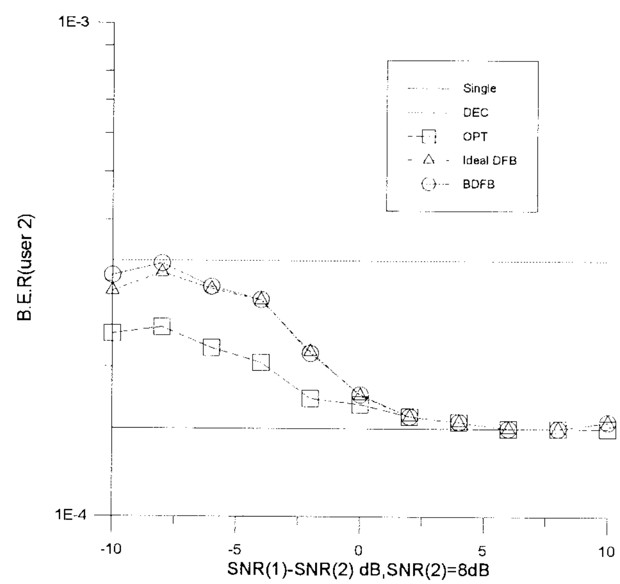

Fig. 7. BER comparison of the BDDF, ideal DDF, decorrelating, single-user, and optimum detectors for a two-user channel with $R_{12} = 1/3$ and signal-to-noise ratio of user 2 fixed at 8 dB.

using LSA is able to achieve the best estimation performance in the fastest convergence rate even though the users are not ranked properly. In other words, our blind adaptation mechanism is independent of the user order.

The BER's were determined by simulating the DDF detector with a blind adaptive energy estimation using LSA for synchronous CDMA AWGN channels and taking an average of 50 individual runs of 10^6 samples. Fig. 7 shows the BER of the second user versus the difference between input signal-to-noise ratios when SNR(2) $= 8$ dB. It is observed that the BER curve of the DDF detector with blind adaptive energy estimation (BDDF) is almost identical to that of the DDF detector with exactly known received energies (ideal DDF) even though the order of two users is interchanged, i.e., SNR(1) $-$ SNR(2) < 0. In other words, P_{ek}(DDF| Blind Energy Estimation) $\approx P_{ek}$(DDF| Ideal Estimation). This implies that our blind energy estimator is able to achieve the best energy estimation performance in the BER manner defined in (15). Note that the ideal DDF detector does not know the order of users. Moreover, both the BDDF and ideal DDF detectors have lower error rate than that of decorrelator of (6). As the first user grows stronger, the BER's of the second user for both the DDF detectors approach the same single-user bound of (9). For the range from 0 to 10 dB, i.e., SNR(1) $>$ SNR(2) (correct order of users), the BER curve of BDDF detector is almost identical to that of the optimum CDMA detector. However, the BER of BDDF detector may be higher than

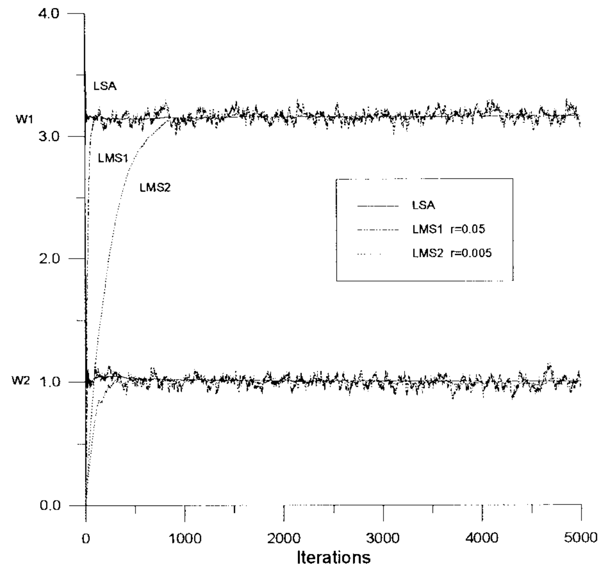

Fig. 8. Comparison of the estimated energies achieved by LSA, LMS1, and LMS2 for a two-user CDMA BDDF detector with $R_{12} = 0.7$ when $w_1 = \sqrt{10},\ w_2 = 1$, (correct user order), and $\sigma^2 = 0.079\,43$.

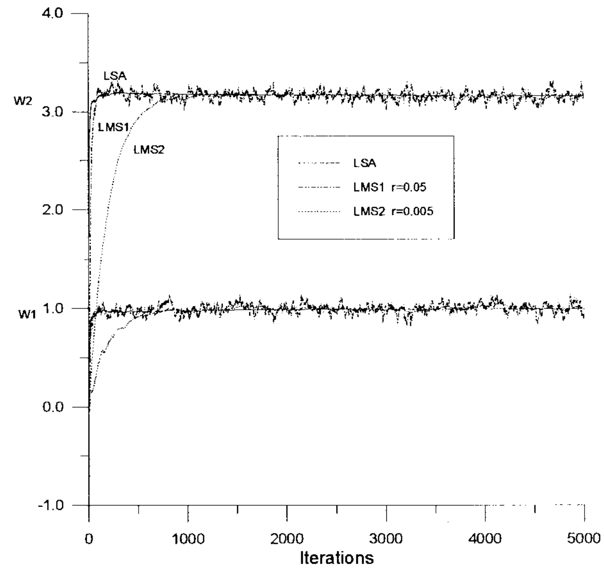

Fig. 10. Comparison of the estimated energies achieved by LSA, LMS1, and LMS2 for a two-user CDMA BDDF detector with $R_{12} = 0.7$ when $w_1 = 1,\ w_2 = \sqrt{10}$, (reverse user order), and $\sigma^2 = 0.079\,43$.

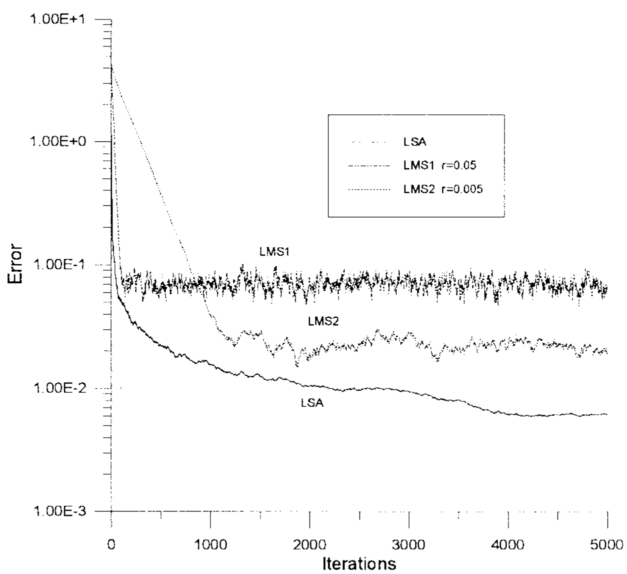

Fig. 9. Comparison of mean square errors achieved by LSA, LMS1, and LMS2 for a two-user CDMA BDDF detector with $R_{12} = 0.7$ when $w_1 = \sqrt{10},\ w_2 = 1$, (correct user order), and $\sigma^2 = 0.079\,43$.

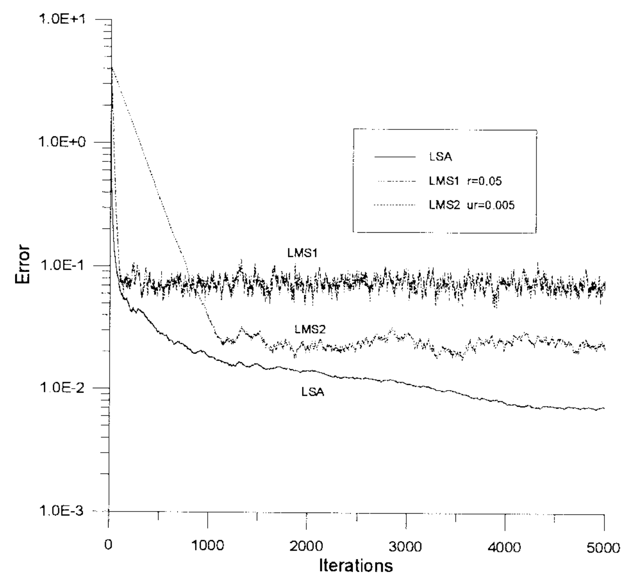

Fig. 11. Comparison of mean square errors achieved by LSA, LMS1, and LMS2 for a two-user CDMA BDDF detector with $R_{12} = 0.7$ when $w_1 = 1,\ w_2 = \sqrt{10}$, (reverse user order), and $\sigma^2 = 0.079\,43$.

that of the optimum CDMA detector for the range from -10 to 0 dB, i.e., SNR(2) $>$ SNR(1) (reverse order of users). Furthermore, the BER of the BDDF detector decreases and finally approaches a single-user bound when SNR(1) (w_1) decreases and is less than a value of -10 dB. Next, we consider the higher bandwidth-efficient two-user synchronous CDMA system with a higher cross correlation $R_{12} = 0.7$. Figs. 3 and 4 depict the convergence curves of the estimated energies and their MSE errors in much the same set up as do Figs. 3 and 4, respectively, when the user order is correct. For the case of reverse user order, Figs. 10 and 11 show their convergence curves which are almost identical to that of Figs. 5 and 6, respectively. Observing Figs. 8–11, LSA achieves the best energy estimation performance in the fastest convergence rate. This again verifies the fact that the blind adaptation mechanism is independent of user order even the cross correlation is high. Fig. 12 shows the BER curve of BDDF detector which is almost identical to that of optimum CDMA detector when the order of users is correct. However, for the case of reverse order, the BER of user 2 for the BDDF detector is higher than that of the decorrelator for the range from -10 to -7.5 dB. Moreover, as SNR(1) (w_1) decreases, the BDDF detector again performs better than the decorrelator and finally approaches the single-user bound. In order to eliminate the case of reverse order, we can apply the two-phase blind adaptation to the BDDF detector. The first-phase adaptation is used to determine the order of users within a specific short time period. Then, after interchanging the order,

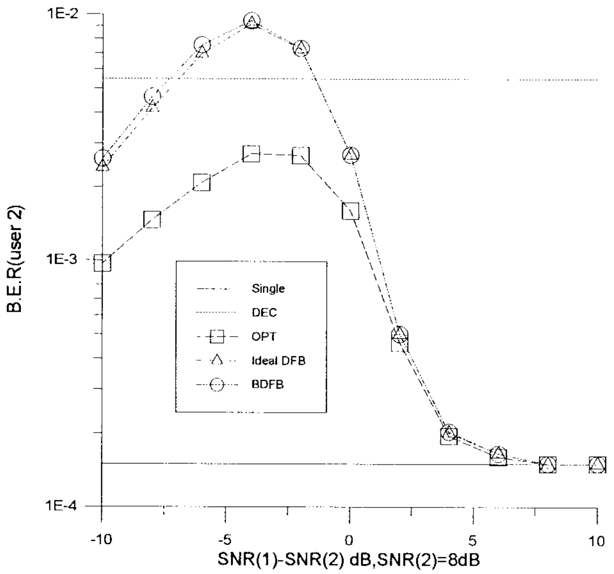

Fig. 12. BER comparison of the BDDF, ideal DDF, decorrelating, single-user, and optimum detectors for a two-user channel with $R_{12} = 0.7$ and signal-to-noise ratio of user 2 fixed at 8 dB.

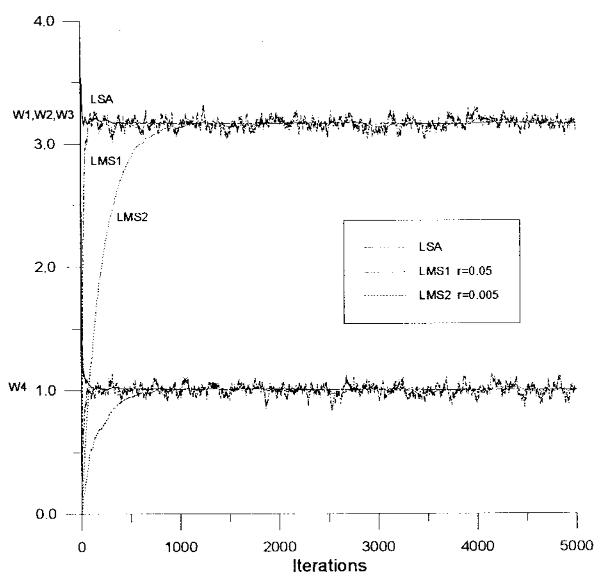

Fig. 13. Comparison of the estimated energies achieved by LSA, LMS1, and LMS2 for a four-user BDDF detector with Gold codes of length 7 when $w_1 = w_2 = w_3 = \sqrt{10},\ w_4 = 1$, (correct user order), and $\sigma^2 = 0.079\,43$.

user 2 becomes the strongest user which performs the same as the decorrelator. However, by performing the second-phase adaptation, user 1 becomes the weakest user whose BER curve coincides with the BER curve for user 2 of Fig. 12 for the range from 0 to 10 dB. Note that user 2 is the weakest user for the range from 0 to 10 dB, however, he becomes the strongest user when the signal-to-noise difference ranges from -10 to 0 dB.

It is of interest to conduct a similar study for a four-user synchronous CDMA system with a set of signature waveforms derived from Gold sequence of length seven, i.e., $a_1(t) = [1,-1,-1,1,1,1,-1]$, $a_2(t) = [1,1,-1,-1,-1,-1,-1]$, $a_3(t) = [1,-1,-1,-1,-1,1,-1]$, and $a_4(t) =$

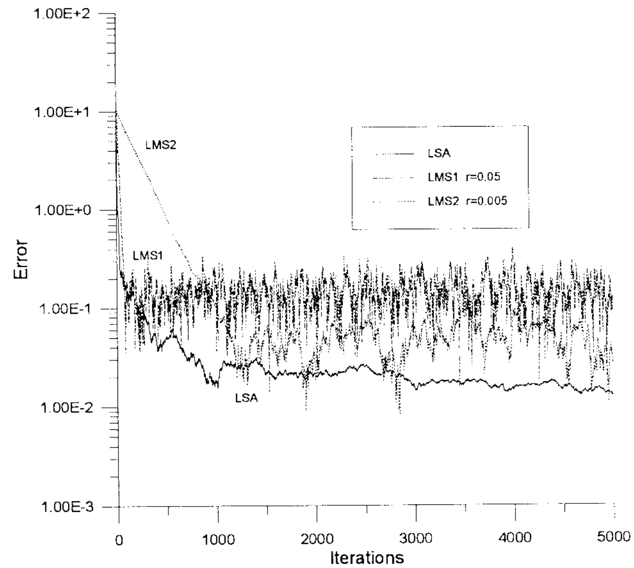

Fig. 14. Comparison of mean square errors achieved by LSA, LMS1, and LMS2 for a four-user BDDF detector with Gold codes of length 7 when $w_1 = w_2 = w_3 = \sqrt{10},\ w_4 = 1$ (correct user order), and $\sigma^2 = 0.079\,43$.

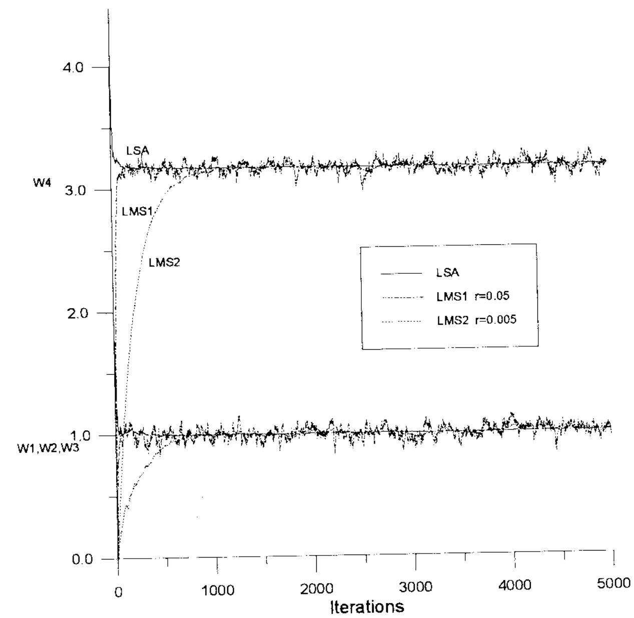

Fig. 15. Comparison of the estimated energies achieved by LSA, LMS1, and LMS2 for a four-user BDDF detector with Gold codes of length 7 when $w_1 = w_2 = w_3 = 1,\ w_4 = \sqrt{10}$ (reverse user order), and $\sigma^2 = 0.079\,43$.

$[-1,1,-1,1,1,1,-1]$. The corresponding cross-correlation matrix is given by

$$R = \frac{1}{7}\begin{bmatrix} 7 & -1 & 3 & 3 \\ -1 & 7 & -1 & 3 \\ 3 & -1 & 7 & -1 \\ 3 & 3 & -1 & 7 \end{bmatrix}. \tag{34}$$

Figs. 13 and 14 illustrate the convergence of the estimated energies and their associated MSE errors achieved by both the LSA and LMS algorithms when $w_1 = w_2 = w_3 = \sqrt{10}, w_4 =$

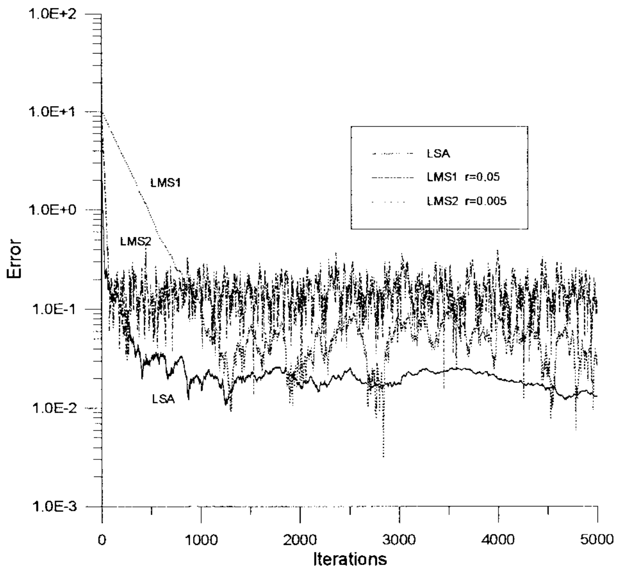

Fig. 16. Comparison of mean square errors achieved by LSA, LMS1, and LMS2 for a four-user BDDF detector with Gold codes of length 7 when $w_1 = w_2 = w_3 = 1,\ w_4 = \sqrt{10}$ (reverse user order), and $\sigma^2 = 0.079\,43$.

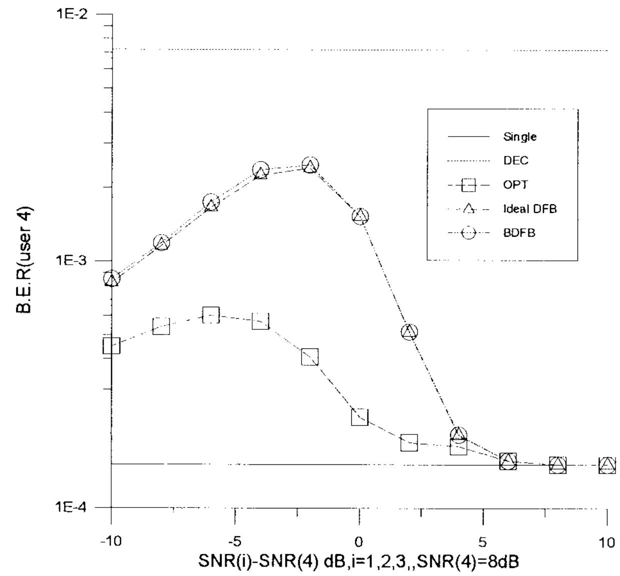

Fig. 17. BER comparison of the BDDF, ideal DDF, decorrelating, single-user, and optimum detectors for a four-user channel with Gold codes of length 7 and signal-to-noise ratio of user 4 fixed at 8 dB.

1, and $\sigma^2 = 0.079\,43$. Both figures show that LSA achieves the best estimation performance in the fastest convergence rate and has a very small variation. However, LMS algorithms have large variations. Especially, Fig. 14 shows that there is an extremely large variation in the learning curve of the LMS algorithm with $r = 0.05$ since the large random variation is resulted from a large sum interference of three interfering users. However, the decreasing harmonic learning sequence of LSA is conducted to eliminate the large random variation. Figs. 15 and 16 show their convergence curves which are almost identical to that of Figs. 13 and 14, respectively. This again verifies that our blind energy estimation is independent of the user order.

The BER's of decorrelator, single-user bound, optimal CDMA detector, ideal DDF (knows all the users' received energies except for their order), and BDDF detector for user 4 are shown in Fig. 17. The input signal-to-noise ratio is SNR(4) $= 8$ dB for user 4 and varies from -2 to 18 dB for other users. We observe that BDDF detector has significantly lower error rate than the decorrelator and coincides with the ideal DDF detector. For the case of correct user order, the BDDF detector almost coincides with the optimum CDMA detector and approaches the single-user bound as interfering users grow stronger. If the users of BDDF detector are not ranked properly, its order may be corrected using the proposed two-phase blind adaptation.

VI. Conclusion

This paper has introduced a new blind energy estimation mechanism for decorrelating DDF multiuser detector which is capable of dealing with the binary SS-CDSMA signals over the synchronous AWGN channel by using learning-type stochastic approximation (LSA) algorithms. This blind energy estimation mechanism using LSA does not require training data. Results show that the LSA algorithm is able to achieve the best estimation performance in a fastest convergence rate even the users of the BDDF detector are not ranked properly. Incorporation of the blind energy estimation using LSA in the DDF structure yields an improved BER performance which is almost identical to that of the DDF detector with exactly known users' energies. Results also show that after performing a two-phase adaptation, the BER curve of the weakest user will coincide with the optimal CDMA BER curve and finally approaches the single-user bound when the interfering users become sufficiently stronger.

References

[1] A. J. Viterbi, *CDMA, Principle of Spread Spectrum Communications*. New York: Addison-Wesley, 1995.

[2] A. Duel-Hallen, J. Holtzman, and Z. Zvonar, "Multiuser detection CDMA systems," *IEEE Personal Commun.*, vol. 2, pp. 46–58, Apr. 1995.

[3] R. Lupas and S. Verdu, "Linear multiuser detectors for synchronous code-division multiple access channels," *IEEE Trans. Inform. Theory*, vol. 35, pp. 123–136, Jan. 1989.

[4] ——, "Near–far resistance of multiuser detectors in asynchronous channels," *IEEE Trans. Commun.*, vol. 38, pp. 496–508, Apr. 1990.

[5] M. K. Varanasi and B. Aazhang, "Near-optimum detection in synchronous code-division multiple-access systems," *IEEE Trans. Commun.*, vol. 39, pp. 725–736, May 1991.

[6] S. Verdu, "Computational complexity of optimum multiuser detection," *Algorithmica*, vol. 4, no. 3, pp. 303–312, 1989.

[7] A. Duel-Hallen, "Decorrelating decision-feedback multiuser detector for synchronous code-division multiple-access channel," *IEEE Trans. Commun.*, vol. 41, pp. 285–290, Feb. 1993.

[8] L. Wei and C. Schlegel, "Synchronous DS-SSMA system with improved decorrelating decision-feedback multiuser detection," *IEEE Veh. Technol.*, vol. 43, pp. 767–772, Aug. 1994.

[9] Z. Xie, R. T. Short, and C. K. Rushforth, "A family of suboptimum detectors for coherent multiuser Communications," *IEEE J. Select. Areas Commun.*, vol. 18, pp. 683–690, May 1990.

[10] T. Kawahara and T. Matsumoto, "Joint decorrelating multiuser detection and channel estimation in asynchronous CDMA mobile communication channels," *IEEE Veh. Technol.*, vol. 44, pp. 506–515, Aug. 1995.

[11] D. S. Chen and S. Roy, “An adaptive multiuser receiver for CDMA system,” *IEEE J. Select. Areas Commun.*, vol. 12, pp. 808–816, June 1994.

[12] M. Honing, U. Madhow, and S. Verdu, “Blind adaptive multiuser detection,” *IEEE Trans. Inform. Theory*, vol. 41, pp. 944–961, July 1995.

[13] S. Bellini and F. Rocca, “Blind deconvolution: Polyspectra or Bussgang techniques,” in *Digital Communications*, E. Biglieri and G. Prati, Eds. New York: North-Holland, 1986, pp. 251–262.

[14] H. Robins and S. Monro, “A stochastic approximation,” *Ann. Math. Stat.*, vol. 22, p. 400, 1951.

[15] A. Dvoretzky, “On stochastic approximation,” in *Proc. 3rd Berkeley Symp. on Math. Stat. and Prob..*, Los Angles, CA, vol. 1, 1956, pp. 39–59.

[16] G. N. Saridis, Z. J. Nikolic, and F. S. Fu, “Stochastic approximation algorithms for system identification, estimation, and decomposition of mixtures,” *IEEE Trans. Syst. Sci. Cybern.*, vol. SSC-5, pp. 8–16, Jan. 1969.

[17] G. N. Saridis, “Learning applied to successive approximation algorithms,” *IEEE Trans. Syst. Sci. Cybern.*, vol. SSC-6, pp. 97–103, Apr. 1970.

Po-Rong Chang (M’87), for a photograph and biography, see this issue, p. 477.

Chih-Chien Lee received the B.S. and M.S. degrees in communication engineering from the National Chiao-Tung University, Hsinchu, Taiwan, R.O.C., in 1994 and 1996, respectively.

He is currently with the National Chiao-Tung University.

Chin-Feng Lin was born in Taiwan, R.O.C., in 1965. He received the B.S. degree in electrical engineering from Chung-Yung University, Chung-Li, Taiwan, in 1996 and the M.S. degree in electrical engineering from Chung-Hua University, Hsinchu, Taiwan, in 1998. He is currently working towards the Ph.D. degree in communication engineering at the National Chiao-Tung University, Hsinchu.

His research interests include CDMA systems and wireless multimedia communications.